

# Phospholipid scramblase 1 is required for $\beta_2$ -glycoprotein I binding in hypoxia and reoxygenation-induced endothelial inflammation

Emily Archer Slone, Michael R. Pope, and Sherry D. Fleming<sup>1</sup>

Division of Biology, Kansas State University, Manhattan, Kansas, USA

RECEIVED OCTOBER 10, 2014; REVISED MAY 26, 2015; ACCEPTED JULY 1, 2015. DOI: 10.1189/jlb.3A1014-480R

## ABSTRACT

Multiple pathologic conditions, including hemorrhage, tumor angiogenesis, and ischemia-reperfusion events, will result in hypoxia and subsequent reperfusion. Previous studies have analyzed the lipid changes within whole tissues and indicated that ischemia-reperfusion altered tissue and cellular phospholipids. Using an *in vitro* cell culture model of hypoxia and reoxygenation, we examined the endothelial lipid changes. We hypothesized that phospholipid scramblase 1, a protein that regulates bilayer asymmetry, is involved in altering the phospholipids of endothelial cells during hypoxia, a component of ischemia, leading to  $\beta_2$ -glycoprotein I and IgM binding and subsequent lipid-mediated, inflammatory responses. We have completed the first comprehensive study of steady-state phospholipid scramblase 1 mRNA levels, protein expression, and activity under conditions of hypoxia and reoxygenation. Phospholipid scramblase 1 regulates phosphatidylserine exposure in response to oxygen stress, leading to  $\beta_2$ -glycoprotein I and IgM binding and lipid-mediated, inflammatory responses. *J. Leukoc. Biol.* 98: 791–804; 2015.

## Introduction

The eukaryotic cell membrane is a mosaic of phospholipids, glycolipids, cholesterol, and other lipid moieties, in addition to the many proteins that associate with the membrane. Previous studies have investigated the intestinal phospholipid composition of wild-type, *Rag-1*<sup>-/-</sup>, and *TLR9*<sup>-/-</sup> mice using mass spectrometry [1, 2]. Although no statistically significant differences in intestinal phospholipids were found between the strains of mice, the phospholipid compositions were altered by IR treatment [1, 2]. The lipid changes included increased production of

lysolipids and AA, which is converted to PGs by the Cox enzymes [1, 3]. Because endothelial hypoxia occurs in multiple pathologic conditions, including IR, hemorrhage, and tumor angiogenesis, we examined the endothelial lipid changes associated with hypoxia.

Production of PGE<sub>2</sub>, a strong vasodilator and mediator of vascular permeability, is necessary, although not sufficient, for IR-induced injury [3]. Numerous studies have reported an increase in PGE<sub>2</sub> production after reoxygenation of an oxygen-deprived tissue. *In vivo* IR studies of the intestine [1, 3] and cerebrum [4, 5] have demonstrated an increase in PGE<sub>2</sub> levels, as have *in vitro* hypoxia studies with neonatal dermal cells [6]. However, the specific cell types involved in the production of PGE<sub>2</sub> during IR is unknown. Hypoxia followed by reoxygenation is frequently used as an *in vitro* model of this damaging clinical condition. It is known that hypoxia stimulates transcription of the inducible Cox isoform, Cox2, which converts AA to PGs in endothelial cells [7]. Importantly, PGE<sub>2</sub> production correlates with PS exposure in erythrocytes [8], and calcium-independent phospholipase A<sub>2</sub> in PS liposomes induces PGE<sub>2</sub> production [9].

The lipid bilayer is asymmetric, with most of the choline-containing phospholipids in the outer leaflet and most of the anionic phospholipids in the inner or cytosolic leaflet (reviewed in [10, 11]). Although lipid bilayers are dynamic and continuously undergoing slight modifications, certain stimuli can induce major changes in the organization of the bilayer. A common end result of bilayer disruption is the exposure of PS, an anionic phospholipid, on the outer leaflet of the cell membrane, which might mark the cell for apoptosis and/or coagulation (reviewed in [12, 13]). Recognition of PS in the outer leaflet by the serum protein,  $\beta_2$ -GPI, might protect the endothelium from oxidative stress and inhibit angiogenesis. However, when bound by antibodies, the complex acts as an opsonin of apoptotic cells [14–16].

Three classes of proteins are responsible for maintaining the asymmetry of the phospholipid bilayer under quiescent conditions (reviewed in [17]). Two of these protein classes, flippases

Abbreviations: AA = arachidonic acid, APS = antiphospholipid syndrome,  $\beta_2$ -GPI =  $\beta_2$ -glycoprotein I, Cox = cyclooxygenase, ESI-MS/MS = electrospray ionization tandem mass spectrometry, HIF-1 $\alpha$  = hypoxia inducible factor-1 $\alpha$ , IR = ischemia and reperfusion, lysoPC = lysophosphatidylcholine, NBD-PS = 1,2-dioleoyl-*sn*-glycero-3-phospho-L-serine-*N*-(7-nitro-2-1,3-benzoxadiazol-4-yl)-labeled phosphatidylserine, NEM = *N*-ethylmaleimide, NL = neutral loss,

(continued on next page)

1. Correspondence: Division of Biology, Kansas State University, 18 Ackert Hall, Manhattan, KS 66506, USA. E-mail: sdflem@ksu.edu

and floppases, require ATP for phospholipid transport. In contrast, scramblases, the third protein class, are ATP independent, responding alternatively to increased cytosolic calcium concentrations ([18–20], reviewed in [17]) or acidic pH [21]. The scramblases are a very likely candidate for involvement in hypoxia-induced phospholipid changes, because hypoxia treatment results in ATP depletion [22, 23], increased acidity [24], and increased concentrations of intracellular calcium ([22, 25], reviewed in [26]). Each of the 4 scramblase proteins localizes to a specific cellular compartment, with PLSCR1 found in the plasma membrane [27].

The present study investigated the hypothesis that endothelial cells are key mediators of the inflammatory response observed after oxygen deprivation. Furthermore, this response can be initiated by PLSCR1-mediated lipid scrambling, allowing for  $\beta_2$ -GPI binding and subsequent inflammation. Because lipidomic analysis of tissues does not determine the specific cell types involved, we used a hypoxia and reoxygenation model to examine the lipid changes within a specific cell population. We report the findings on the steady-state mRNA and protein expression and activity of PLSCR1 under hypoxic conditions. The effects of hypoxia and reoxygenation on  $\beta_2$ -GPI and IgM binding, phospholipid changes, and downstream inflammatory markers in endothelial cells are also demonstrated. Our results confirm that endothelial cells contribute to the inflammatory response observed after a period of hypoxia and are likely intimately involved in the tissue damage observed after IR. Furthermore, PLSCR1 appears to facilitate early phospholipid changes in endothelial cells that ultimately result in a tissue inflammatory response.

## MATERIALS AND METHODS

### Cells

The mouse (C57Bl/6) endothelial cell line, MS1 (American Type Culture Collection, Manassas, VA, USA), was grown and maintained in Dulbecco's modified Eagle medium (Gibco, Grand Island, NY, USA) with 10% fetal bovine serum (Atlanta Biologicals, Lawrenceville, GA, USA), 10% Opti-MEM (Gibco), and 1% Gluta-MAX (Gibco) in a humidified 5% CO<sub>2</sub> incubator.

### Hypoxia

The cells were seeded ( $3 \times 10^6$  for lipid and PGE<sub>2</sub> analysis,  $1 \times 10^6$  for RNA extraction, and  $1 \times 10^7$  for Western blot) on tissue culture plates for 12–18 h before hypoxia treatment. At the experiment, the medium was replaced with medium that had been deoxygenated, either by 5 min of bubbling with a 9.989% O<sub>2</sub>, 5.070% CO<sub>2</sub>, 93.941% N<sub>2</sub> gas mixture (referred to as 1% O<sub>2</sub>) or placing the medium under vacuum for 15 min in a sealed flask. Plates of cells were transferred to a hypoxia chamber (modular incubator chamber; Billups-Rothenburg, Inc., Del Mar, CA, USA), and the chamber was purged with the same gas mixture at 20 L/min for 5 min. The chamber was held at 37°C for 2 h. After 2 h of hypoxia, the cells were removed from the hypoxia chamber, the hypoxic medium was replaced with normoxic medium, and cells were placed into normoxic culture conditions (37°C humidified incubator with 5%

(continued from previous page)

PC = phosphatidylcholine, PE = phosphatidylethanolamine, PI = phosphatidylinositol, PLSCR1 = phospholipid scramblase 1, PS = phosphatidylserine, QRT-PCR = quantitative real-time PCR, siRNA = small interfering RNA, SLE = systemic lupus erythematosus, TCPBS = tissue culture phosphate-buffered saline, TKI = tyrosine kinase inhibitor, VEGF = vascular endothelial growth factor

CO<sub>2</sub>). The cells then were collected 15, 30, or 60 min later. Normoxic-treated cells were subjected to normal growth conditions with replacement of normoxic medium at the beginning of the experiment and again after 2 h.

### PGE<sub>2</sub>

After normoxic or hypoxic treatment, supernatants were collected from the cells and stored at –80°C until assayed. The PGE<sub>2</sub> concentration was determined using a PGE<sub>2</sub> Express EIA Kit (Cayman Chemical, Ann Arbor, MI, USA) and expressed as picograms per milliliter.

### Lipid Extraction

Lipids were extracted using a method similar to that described previously [1]. In brief, after normoxic or hypoxic treatment, medium was removed, and the cells were lysed with distilled water. The cells were then collected from the tissue culture plates, and lysates were stored at –80°C until lipid extraction. The lysates were thawed, vortexed, and transferred to glass tubes that had been washed with a cation/phosphate-free liquid detergent (Contrex, Decon Labs, King of Prussia, PA, USA) to eliminate contamination. Next, 1 ml of chloroform and 2 ml of methanol were added, and the tubes were shaken vigorously. An additional 1 ml of chloroform and 1 ml of distilled water were added, and the tubes were again shaken vigorously. The tubes were centrifuged at 4000 rpm for 5 min at 4°C. The organic layers were transferred to clean glass tubes, and 1 ml of chloroform added to the aqueous phase. The tubes were again shaken and centrifuged, and the organic layers were removed 2 additional times. Distilled water (0.5 ml) was added to the combined organic layers from each sample, and each was centrifuged once more. The samples (organic layers) were submitted to the Kansas Lipidomics Research Center for analysis by mass spectrometry.

### Mass Spectrometry

An automated ESI-MS/MS approach was used, and data acquisition and analysis were performed at the Kansas Lipidomics Research Center, as described previously, with some modifications [28, 29]. Solvent was evaporated from the extracts, and each sample was dissolved in 1 ml of chloroform. Precise amounts of internal standards, obtained and quantified as previously described [30], were added to the sample to be analyzed. The sample and internal standard mixture were combined with solvents, such that the ratio of chloroform to methanol to 300 mM ammonium acetate in water was 300:665:35, and the final volume was 1.2 ml. These unfractionated lipid extracts were introduced by continuous infusion into the ESI source of a triple quadrupole MS/MS (API 4000; Applied Biosystems, Foster City, CA, USA) using an autosampler (LC Mini PAL; CTC Analytics AG, Zwingen, Switzerland) fitted with the required injection loop for the acquisition time and presented to the ESI needle at 30  $\mu$ l/min.

Sequential precursor and neutral loss scans of the extracts produced a series of spectra, with each spectrum revealing a set of lipid species containing a common head group fragment. Lipid species were detected with the following scans: PC, sphingomyelin and lysoPC, [M + H]<sup>+</sup> ions in positive ion mode with precursor of 184.1; PE and lysoPE, [M + H]<sup>+</sup> ions in positive ion mode with NL of 141.0; PI, [M + NH<sub>4</sub>]<sup>+</sup> in positive ion mode with NL 277.0; PS, [M + H]<sup>+</sup> in positive ion mode with NL 185.0; phosphatidic acid, [M + NH<sub>4</sub>]<sup>+</sup> in positive ion mode with NL 115.0; PG, [M + NH<sub>4</sub>]<sup>+</sup> in positive ion mode with NL 189.0; lysophosphatidylglycerol, [M – H]<sup>–</sup> in negative mode with Pre 152.9; and free fatty acids (i.e., free AA), [M – H]<sup>–</sup> in negative mode with single-stage MS analysis. For each spectrum, 9–150 continuum scans were averaged in multiple channel analyzer mode.

The background of each spectrum was subtracted, the data were smoothed, and the peak areas were integrated using a custom script and Applied Biosystems Analyst software (Applied Biosystems, Carlsbad, CA, USA). The lipids in each class were quantified in comparison with the 2 internal standards of that class, except for PI and AA, for which single standards were used. The first and typically every 11th set of mass spectra were acquired on the internal standard mixture only. Peaks corresponding to the target lipids in these spectra were identified and the molar amounts calculated compared with the internal

standards of the same lipid class. To correct for chemical or instrumental noise in the samples, the molar amount of each lipid metabolite detected in the “internal standards only” spectra was subtracted from the molar amount of each metabolite calculated in each set of sample spectra. The data from each “internal standards only” set of spectra were used to correct the data from the subsequent 10 samples. Finally, the data are expressed as the mole percentage of total lipid analyzed. Each class of lipid was also normalized to the sample protein content and expressed as nanomoles of lipid class per milligram of protein.

### Real-Time PCR

After normoxic or hypoxic treatment, the medium was removed and the cells washed once with TCPBS (136.8 mM NaCl, 1.47 mM  $\text{KH}_2\text{PO}_4$ , 2.68 mM KCl, 8.58 mM  $\text{Na}_2\text{HPO}_4 \cdot 7\text{H}_2\text{O}$ ). The cells were collected in 0.5–1 ml of TRIzol Reagent (Invitrogen, Carlsbad, CA, USA), and total RNA was extracted according to the manufacturer’s protocol. Complementary DNA was reverse transcribed from 1  $\mu\text{g}$  extracted RNA using the RevertAid First Strand cDNA Synthesis Kit (Fermentas, Glen Burnie, MD, USA) or Quanta qScript cDNA kit (Quanta BioSciences, Gaithersburg, MD, USA) and made according to the manufacturer’s protocol using random hexamers. Quantitative real-time PCR was used to assess the steady-state mRNA transcript levels. Either Maxima SYBR (Fermentas) or PerfeCTa SYBR Green FastMix (Quanta BioSciences) was used as the master mix (25  $\mu\text{l}$  total volume). The primers used are listed in Table 1 and were obtained from Integrated DNA Technologies (Coralville, IA, USA). The genes of interest were normalized to 18s rRNA of each sample, and the fold change was determined in relation to the normoxic controls.

### Western Blot

Cell lysates were prepared after various lengths of normoxia after 2 h of hypoxia and from normoxic controls. The cells were lysed and stored in a buffer of 10 mM Tris-HCl (pH 7.0), 200 mM NaCl, 5 mM EDTA, 10% glycerol, 1% Nonidet P40 with the following protease inhibitors: AEBSF ( $2 \times 10^{-7}$  M), aprotinin (1  $\mu\text{g}/\text{ml}$ ), leupeptin (10  $\mu\text{g}/\text{ml}$ ), pepstatin (2.5  $\mu\text{g}/\text{ml}$ ), calpain inhibitor (17  $\mu\text{g}/\text{ml}$ ), chymostatin (2.5  $\mu\text{g}/\text{ml}$ ), and antipain (2.5  $\mu\text{g}/\text{ml}$ ). The protein concentration was determined by the bicinchoninic acid assay (Pierce, Rockford, IL, USA) adapted for microtiter plates, and 60  $\mu\text{g}$  of protein was loaded per well on a 10% SDS gel. After transfer to a polyvinylidene difluoride membrane, the membrane was blocked and probed with rabbit anti-PLSCR1 Ab (Proteintech Group, Chicago, IL, USA) at 1:1000 dilution or mouse anti- $\alpha$ -tubulin Ab (GenScript, Piscataway, NJ, USA) at 1:10,000 dilution. Peroxidase-conjugated goat anti-rabbit IgG (Thermo Fisher Scientific, Rockford, IL, USA) and peroxidase-conjugated donkey anti-mouse IgG (Jackson ImmunoResearch Laboratories, West Grove, PA, USA) were used as secondary Abs at a dilution of 1:2500. Blots were visualized with SuperSignal West Pico ECL Substrate (Thermo Fisher Scientific) and developed with an ECOMAX film developer (Protec Medical Devices, Bonn, Germany). ImageJ (NIH, Bethesda, MD, USA) was used to quantify the results, and the average of 5 independent sets of lysates are presented.

### Immunocytofluorescence Staining

The cells were seeded ( $1.5 \times 10^5$  per chamber) on 8 chamber glass slides (BD Falcon, Franklin Lakes, NJ, USA) and allowed to adhere for 2 h or overnight. The medium was replaced with serum free deoxygenated medium, as described, and the slides were placed in a hypoxia chamber for 2 h or remained in normal culture conditions as normoxic controls. After hypoxia, the cells were provided with fresh medium, and reoxygenation was allowed for 1 h in the presence of 10% Rag-2<sup>-/-</sup> ( $\beta_2$ -GPI) or C57Bl/6 (IgM) serum. The cells were then fixed with methanol and blocked with 10% normal donkey sera for 30 min at 37°C. The cells were stained overnight at 4°C with anti-human  $\beta_2$ -GPI Ab (R&D Systems, Minneapolis, MN, USA, or EMD Millipore, Billerica, MA, USA) or with donkey anti-IgG and IgM (3  $\mu\text{g}/\text{ml}$ ) directly conjugated with FITC or Alexa Fluor 594, respectively (Jackson ImmunoResearch Laboratories, West Grove, PA, USA) at concentrations recommended by the manufacturer. FITC-conjugated donkey anti-goat IgG Ab (Jackson ImmunoResearch Laboratories) was used as a secondary Ab for the anti- $\beta_2$ -GPI Ab. Appropriate isotype control Abs were used, and the slides were mounted with Prolong Gold containing DAPI (Invitrogen). A Nikon Eclipse 80i microscope with CoolSnap CF camera (Photometrics, Tucson, AZ, USA) and Metavue software (Molecular Devices, Sunnyvale, CA, USA) were used to obtain images at room temperature.

### Labeled Lipid Experiments

The cells were seeded ( $1.5 \times 10^5$ ) on glass coverslips and allowed to adhere for 2–4 h. During this time, a solution containing NBD-PS (Avanti Polar Lipids, Alabaster, AL, USA; 1  $\mu\text{M}$  lipid, 5.5 mM dextrose in TCPBS) was added at a dilution of 1:100 to the medium to allow for lipid incorporation. The thio-modifying agent, which also inhibits flippases, NEM (Alfa Aesar, Ward Hill, MA, USA) was added to the coverslips at a concentration of 5 mM for the final 30 min. The inhibitor NEM was removed, and the cells were treated with hypoxia, as described. After hypoxic or normoxic treatment, the cells were rinsed with TCPBS and fixed with ice-cold methanol for 3 min. Trypan blue (0.4%) was added to selected coverslips for 30 s to quench fluorescence in the outer leaflet. After additional TCPBS washes to remove excess lipid, the coverslips were mounted on glass slides with Prolong Gold containing DAPI (Invitrogen). Parallel experiments were performed without the inhibitor NEM. A Nikon Eclipse 80i microscope with CoolSnap CF camera (Photometrics) and Metavue software (Molecular Devices) were used to obtain images at room temperature.

### siRNA Transfection

The transfection protocol provided by manufacturer (Santa Cruz Biotechnology, Inc., Dallas, TX, USA) was followed. In brief, the cells were seeded into 6-well plates at a density of  $2 \times 10^5$  cells per well. Next, 5  $\mu\text{l}$  of siRNA duplex (a pool of 3 PLSCR1-specific siRNAs or scrambled control siRNAs, each 20–25 nucleotides long) and 5  $\mu\text{l}$  of siRNA transfection reagent were used to prepare solutions A and B, respectively. Solutions A and B were mixed and allowed to

TABLE 1. QRT-PCR primer sequences

Gene	$T^a$ (°C)	Primer sequence	
		Forward	Reverse
18s <sup>b</sup>	58	GGTTGATCCTGCCAGTAGC	GCGACCAAAGGAACCATAAC
VEGF	57	AGAGCAACATCACCATGCAG	TTTCTTGGCTTTTCGTTTTT
Flt-1	56	TATAAGGCAGCGGATTGACC	TCATACACATGCACGGAGGT
COX1	56	AAGGAGTCTCTCGCTCTGCTTT	TCTCAGGATGGTACAGTTGGG
COX2	58	ATTCAACACACTCTATCACTGGC	CTGGTAATTCATCTCTCTGCTCTG
PLSCR1	56	TAGCTGCTGTTCCGACATTG	ACAAGCACAAGCATCACAG
PLSCR3	57	GTTACCACATCTCCAGGCAGT	TAAGGGAAGGGTGGTGTCTG
Atp8a1 (flippase)	56	GTGTTTTGCTGTGGCTGAGA	ATGTTTTCAGGCACTTGCTC
Abcb1a (floppase)	56	GGCTTACAGCCAGCATTTCTC	CCAGCTCACATCCTGTCTCA

$T$ , temperature. <sup>a</sup>Annealing temperature. <sup>b</sup>Ribosomal RNA; house-keeping gene to which genes of interest were normalized.

incubate at room temperature for 30 min before their addition to the cells. The cells were exposed to transfection medium for 6 h before the addition of the serum-containing medium. The cells were assayed approximately 24 h later. A fraction of the cells from each transfected well was collected either in TRIzol reagent or as a cell lysate. RNA knock down was assessed by real-time PCR as described, and decreased protein expression was assessed by Western blot analysis of PLSCR1 expression. The other portion of each well was used for labeled lipid experiments or immunocytochemistry, as described.

### Annexin V binding

MS1 cells ( $1.5\text{--}2 \times 10^5$  cells per well) were allowed to adhere for 1 h before subjecting the cells to 2 h of hypoxia followed by 30 min of normoxia, as indicated in Hypoxia above, in the presence or absence of the pan-caspase inhibitor, Z-VAD-FMK (20  $\mu\text{M}$ ; R&D Systems) or DMSO as a solvent control. Additional control wells were subjected to normoxia or received 5% ethanol. The cells were removed from the plates, washed into Annexin Binding buffer, and stained with FITC-AnnexinV (BioLegend, San Diego, CA, USA) per the manufacturer's direction for 15 min at room temperature. The washed cells were resuspended in 100  $\mu\text{l}$  of binding buffer and placed on slides by a cytospin. The slides were rinsed and coverslipped and examined as indicated using fluorescent microscopy.

### Statistical analysis

Data are presented as the mean  $\pm$  standard error of the mean. Significance ( $P < 0.05$ ) was determined using one-way analysis of variance with Newman-Keuls post hoc analysis (GraphPad Prism 5; GraphPad Software, Inc., La Jolla, CA, USA), unless otherwise noted.

## RESULTS

### Two hours of hypoxia treatment induces transcription of *HIF* and regulated genes

Previous studies have demonstrated that intestinal tissue from wild-type mice express HIF-1 $\alpha$  in response to IR; however, the specific cell type involved was unknown [31]. To evaluate the role of the endothelium in this inflammatory process, we initially determined an appropriate length of hypoxia treatment to induce HIF-1 $\alpha$  expression in an endothelial cell line, MS1, derived from a C57Bl/6 mouse. Cell viability and transcription of *HIF-1 $\alpha$*  and the genes regulated by *HIF* were assessed. We examined the transcript levels of HIF-1 $\alpha$  and found that exposure to 1% O<sub>2</sub> for 2 h significantly increased the transcription level of *HIF-1 $\alpha$*  ( $1.0 \pm 0.33$  normoxia vs.  $1.84 \pm 0.50$  hypoxia) and that *HIF-1 $\alpha$*  returned to baseline within 60 min of reoxygenation (Fig. 1A). Importantly, cell viability was approximately 88% after 2 h of hypoxia but decreased sharply as the length of hypoxic treatment increased further (data not shown). We also examined genes downstream of *HIF-1 $\alpha$* , including *VEGF* and *Flt-1* (*VEGFR1*), as markers of hypoxia, because the transcription of these genes is induced by hypoxia [32–35]. Similar to *HIF-1 $\alpha$* , hypoxia induced a significant increase in steady-state mRNA of both *VEGF* ( $1.00 \pm 0.19$  normoxia vs.  $2.11 \pm 0.30$  hypoxia) and *Flt-1* ( $1.00 \pm 0.28$  normoxia vs.  $2.50 \pm 0.21$  hypoxia), as determined by QRT-PCR (Fig. 1B). Thus, a hypoxic period of 2 h was used for the remainder of the studies.

### Reoxygenation of endothelial cells generates lipids involved in inflammation

To determine whether hypoxia altered the lipid composition of the endothelial cells similar to what occurs with ischemia, we used ESI-MS/MS to analyze the cells treated with 2 h of hypoxia alone,

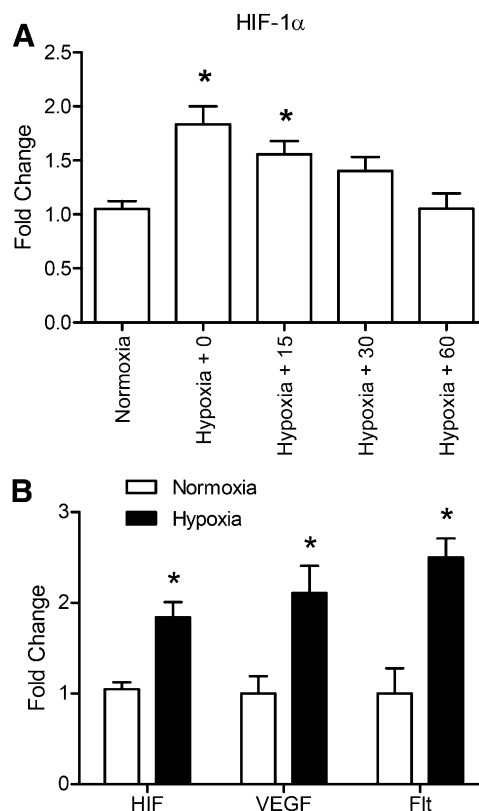


**Figure 1. Hypoxia increases steady-state *HIF-1 $\alpha$*  mRNA.** MS1 cells were subjected to 2 h of hypoxia (1% O<sub>2</sub>) followed by reoxygenation or left in normal culture conditions (N). Fold change in steady-state mRNA expression was determined by QRT-PCR. After hypoxia, followed by 0, 15, 30, or 60 min of reoxygenation, *HIF-1 $\alpha$*  (A) and *VEGF* and *Flt* after normoxia or hypoxia without reoxygenation (B). The results were normalized to the corresponding *18s* rRNA and compared with normoxic samples.  $N = 4\text{--}5$  samples per bar. \* $P < 0.05$  compared with N.

cells treated with 2 h of hypoxia followed by varying lengths of reoxygenation, and cells remaining in normal culture conditions. Although the overall phospholipid composition was not changed after treatment (Table 2), a significant increase in lysoPC was found during the reoxygenation period (Fig. 2A). PC did not significantly decrease; however, the abundance of this phospholipid could have easily masked small changes in quantity (Fig. 2B).

We also evaluated the free fatty acid content of the cells, with a special interest in free AA. The increased lysoPC observed with reoxygenation (Fig. 2A) implies phospholipase activity during this period, and a source of free AA is its cleavage from a phospholipid by a phospholipase. Mass spectrometry analysis indicated a decrease in the free AA content of the cells with reoxygenation (Fig. 2C), suggesting possible conversion of newly released AA to eicosanoids, such as PGE<sub>2</sub>, because hypoxia and reoxygenation promotes increased transcription of the Cox enzymes and production of PGE<sub>2</sub> [36].

### Hypoxia and reoxygenation promotes increased transcription of the Cox enzymes and production of PGE<sub>2</sub> by endothelial cells

The lipid findings, in particular, the decrease in free AA, led us to examine the Cox enzymes and production of PGE<sub>2</sub>, because

**TABLE 2. Lipid composition of MS1 endothelial cells with hypoxia and reoxygenation treatment**

Lipid class <sup>a</sup>	Normoxia <sup>b</sup>	0 min <sup>c</sup>	15 min <sup>d</sup>	30 min <sup>e</sup>	60 min <sup>f</sup>
LysoPC	0.04 ± 0.01	0.02 ± 0.00*	0.06 ± 0.00*	0.08 ± 0.01*	0.04 ± 0.01
PC	7.80 ± 0.90	7.82 ± 1.31	8.42 ± 1.21	8.95 ± 1.32	8.59 ± 1.33
SM	1.06 ± 0.20	1.18 ± 0.45	1.34 ± 0.41	1.70 ± 0.46	1.42 ± 0.42
LysoPE	0.03 ± 0.01	0.02 ± 0.01	0.03 ± 0.01	0.04 ± 0.01	0.02 ± 0.00
PE	1.28 ± 0.32	1.61 ± 0.67	2.10 ± 0.67	2.50 ± 0.74	2.18 ± 0.83
PI	0.33 ± 0.09	0.38 ± 0.19	0.38 ± 0.14	0.54 ± 0.18	0.37 ± 0.14
PS	0.21 ± 0.05	0.31 ± 0.11	0.30 ± 0.09	0.47 ± 0.10	0.34 ± 0.09
PA	0.03 ± 0.01	0.02 ± 0.01	0.03 ± 0.01	0.03 ± 0.01	0.03 ± 0.01
PG	0.05 ± 0.01	0.05 ± 0.01	0.07 ± 0.01	0.07 ± 0.02	0.07 ± 0.02

Data are presented as the means ± SEM of nanomoles of lipid per milligram protein after normalization of signal to internal standards of each lipid class. PA, phosphatidic acid; PG, phosphatidylglycerol; SM, sphingomyelin. <sup>a</sup>Lipids were extracted from MS1 endothelial cells after being subjected to 2 h of hypoxia with or without varying lengths of reoxygenation or normoxic culture conditions and subjected to analysis by MS. Each treatment group included 6–9 individual samples. <sup>b</sup>Normoxic controls. <sup>c</sup>Two hours of hypoxia + 0 min of reoxygenation. <sup>d</sup>Two hours of hypoxia + 15 min of reoxygenation. <sup>e</sup>Two hours of hypoxia + 30 min of reoxygenation. <sup>f</sup>Two hours of hypoxia + 60 min of reoxygenation. \*Statistically significant difference ( $P < 0.05$ ) from normoxic controls.

PGE<sub>2</sub>, a modulator of inflammation, is a necessary component for intestinal IR-induced damage [3]. We used QRT-PCR to determine the change in steady-state mRNA of 2 *Cox* isoforms in normoxia and hypoxia/reoxygenation-treated cells. The steady-state transcript of *Cox2*, the inducible isoform, was significantly elevated during the hypoxic period and continued to increase,

with a peak at 30 min of reoxygenation (Fig. 2D). Surprisingly, a significant increase in *Cox1*, considered the constitutive isoform, was also observed and followed the trend of *Cox2* (Fig. 2E). Furthermore, the fold change of *Cox1* exceeded that of *Cox2* (Fig. 2D and E). These data indicate that both isoforms could be involved in PG regulation during periods of hypoxic stress.

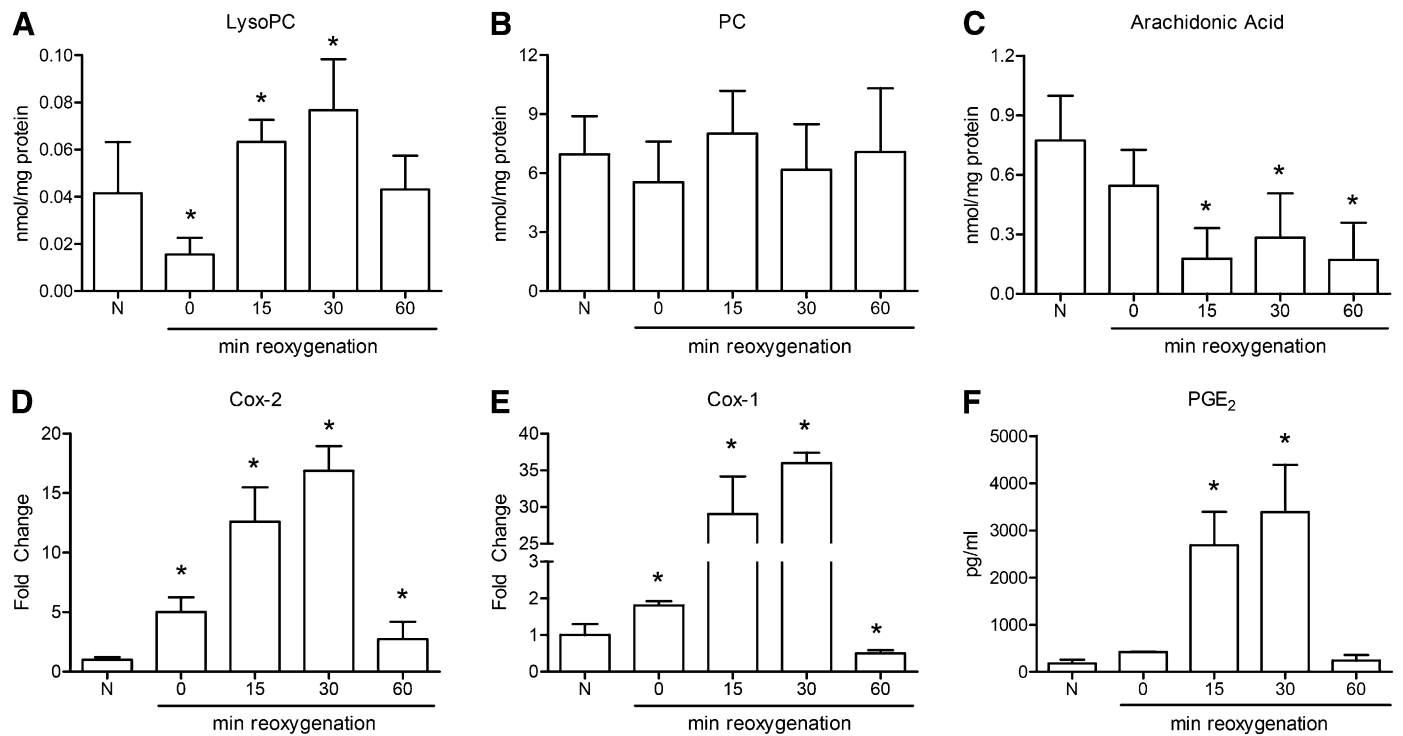


**Figure 2. Lipid-mediated contents change with hypoxia treatment.** A–C) MS1 cells were subjected to 2 h of hypoxia (1% O<sub>2</sub>) followed by 0, 15, 30, or 60 min of normoxia or left in normal culture conditions (N). Lipid content was determined by ESI-MS/MS and normalized to protein content of each sample.  $N = 5$ –9 samples per bar. D–F) Fold change in steady-state mRNA was determined by QRT-PCR. *Cox2* (D) and *Cox1* (E) results were normalized to corresponding 18s rRNA and compared with normoxic samples.  $N = 4$ –5 samples per bar. F) PGE<sub>2</sub> concentration of supernatants produced by  $3 \times 10^6$  cells as determined by enzyme immunoassay.  $N = 3$ –6 samples per bar. \* $P < 0.05$  compared with N.

We continued to investigate our hypothesis by quantifying PGE<sub>2</sub> production. A time course was established to determine whether PGE<sub>2</sub> was produced during the hypoxic period or only on reoxygenation and to identify the time point of maximal response. The endothelial cells significantly upregulated production of PGE<sub>2</sub> on reoxygenation, but no change was seen during the hypoxic period (Fig. 2F). As early as 15 min after hypoxia, the cells significantly increased PGE<sub>2</sub> production compared with the control cells maintained in normal culture conditions. Based on our sampling time points, the production of PGE<sub>2</sub> peaked at 30 min after hypoxia. At that point, the hypoxia-treated cells showed an almost 1800% increase ( $3391 \pm 575$  pg/ml at 30 min of reoxygenation vs.  $179 \pm 33$  pg/ml for normoxic controls) in PGE<sub>2</sub> production compared with normoxic-treated cells. The time course of Cox transcription and PGE<sub>2</sub> production correlate, in that steady-state transcription of Cox enzymes is increased during hypoxia and a significant increase in PGE<sub>2</sub> is not observed until 15 min into the reoxygenation period (Fig. 2D–F). Together, these data indicate that a biologic effect (PGE<sub>2</sub> production) accompanies the lipid composition changes.

**Lipids translocate between leaflets of the hypoxic endothelial cell membrane**

Because hypoxia results in lipid changes, it was likely that lipids were also translocating between the inner and outer leaflets of the cell membrane. This movement was confirmed by 2 methods, β<sub>2</sub>-GPI and annexin V binding. Previous studies have indicated that β<sub>2</sub>-GPI, a serum protein, binds anionic lipids, normally on the inner leaflet of the lipid bilayer, on the endothelium after a period of hypoxia and reoxygenation [37]. To confirm our previous results, endothelial cells were subjected to hypoxia treatment for 2 h followed by 1 h of reoxygenation before analysis by immunocytofluorescence staining. As shown in Fig. 3A, anti-β<sub>2</sub>-GPI Ab stained the hypoxia-treated cells to a much greater extent than did the normoxic control cells. Because β<sub>2</sub>-GPI has been proposed to bind to PS [38], additional studies demonstrated that after hypoxia but not with normoxia, annexin V also bound to the cell surface (Fig. 3B). This binding was similar to that of apoptotic cells that had been treated with 5% ethanol. Propidium iodide was used to demonstrate that the cells remained viable (data not shown). To further rule out apoptosis after hypoxia and reoxygenation, the pan-caspase inhibitor, Z-VAD-FMK, was added to some cultures. As demonstrated in Fig. 3B, Z-VAD-FMK treatment inhibited annexin V binding on ethanol-treated cells but annexin V bound similarly to hypoxia-treated cells in the presence or absence of Z-VAD-FMK. These data indicate that PS is expressed on the cell surface after hypoxia and reoxygenation and is not inhibited by the pan-caspase inhibitor at the early time point. In addition, not only do lipid changes occur, but lipid translocation also occurs between the inner and outer leaflets of the hypoxic endothelial cell membrane.

**Recovery from oxygen deprivation selectively upregulates steady-state PLSCR1 mRNA**

Phospholipids are involved in facilitating both β<sub>2</sub>-GPI binding and the AA cascade. PGE<sub>2</sub> production and PS exposure seem to

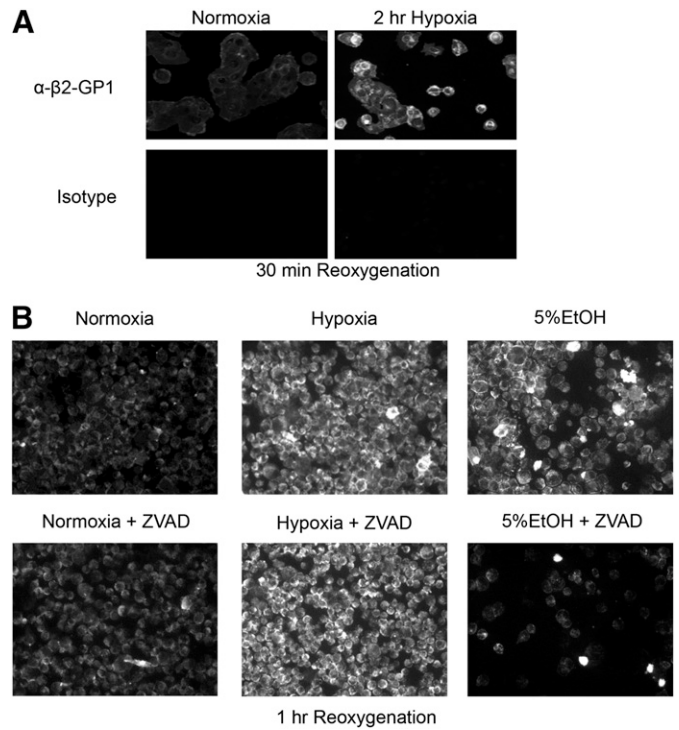


**Figure 3. β<sub>2</sub>-GPI binds endothelium after hypoxia treatment.** A) MS1 cells were grown on chamber slides, subjected to 2 h of hypoxia (1% O<sub>2</sub>), followed by 60 min of reoxygenation or left in normal culture conditions. The cells were fixed and stained for β<sub>2</sub>-GPI binding or negative control (isotype). B) After normoxia, hypoxia followed by 30 min of reoxygenation, or treatment with 5% ethanol (positive control), the cells were incubated with annexin V. Additional cells were treated with Z-VAD during the final 30 min. Images are representative of 3 independent experiments with 4–6 pictures per treatment group per experiment.

be an interactive process, but the mechanism by which the phospholipids change in hypoxic conditions is unknown. Several enzymes play a role in maintaining the asymmetry of the lipid bilayer. We hypothesized that PLSCR1 is involved in mediating the lipid changes that occur with hypoxia and reoxygenation. Analysis by QRT-PCR revealed a significant increase in steady-state *PLSCR1* mRNA in endothelial cells recovering from hypoxia treatment compared with the normoxic control cells (Fig. 4A). Additional phospholipid-transporting proteins were examined to verify that the response of *PLSCR1* to hypoxia and reoxygenation is specific. Steady-state levels of *PLSCR3* mRNA, which localizes to the mitochondrial membrane, did not change with hypoxia but decreased with reoxygenation (Fig. 4C). Similarly, 2 h of hypoxia alone did not alter the steady-state mRNA of the representative flippase (*Atp8a1*) and floppase (*Abcb1a*) proteins. However, reoxygenation decreased the measured mRNA levels (Fig. 4B and D).

**Hypoxia alters PLSCR1 protein expression**

Our QRT-PCR data indicated increased transcription of *PLSCR1*, and we hypothesized that *PLSCR1* protein levels might also increase with reoxygenation. To examine a change in *PLSCR1* protein, whole cell lysates were prepared from hypoxia-treated

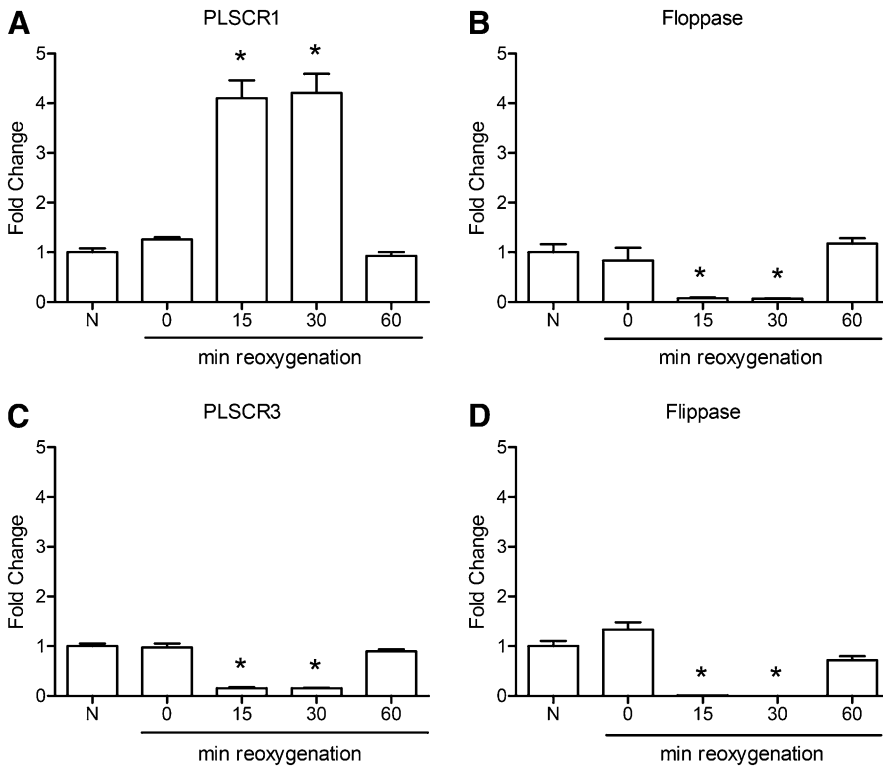


**Figure 4. Hypoxia selectively increases steady-state PLSCR1 mRNA.** MS1 cells were subjected to 2 h of hypoxia (1% O<sub>2</sub>) followed by 0, 15, 30, or 60 min of normoxia or left in normal culture conditions (N). Fold change in steady-state mRNA of *PLSCR1* (A), floppase *Abcb1a* (B), *PLSCR3* (C), and flippase *Atf8a1* (D) was determined by QRT-PCR. Genes of interest were normalized to corresponding *18s* rRNA and compared with normoxic samples. N = 4–5 samples per bar. \**P* < 0.05 compared with N.

and normoxic control endothelial cells. Western blot analysis indicated a decrease in PLSCR1 protein levels immediately after 2 h of hypoxia treatment (time 0–30 min) compared with normoxic controls, with the change being statistically significant at the time points of 0, 15, and 30 min (Fig. 5). The protein levels tended to increase back toward normoxic levels as reoxygenation proceeded (Fig. 5). Taken together, our data indicate that the PLSCR1 protein decreases during the hypoxic period but that reoxygenation induces an upregulation in steady-state mRNA

and decreases the protein expression for the first 15–30 min (Figs. 4A and 5). These data suggest that PLSCR1 is sensitive to oxygen tension and might be involved in the phospholipid changes that occur in response to hypoxia and reoxygenation.

**Hypoxia and reoxygenation increases activity of PLSCR1**

Changes in transcription and total protein do not necessarily correlate with protein activity. Thus, we assayed for PLSCR1

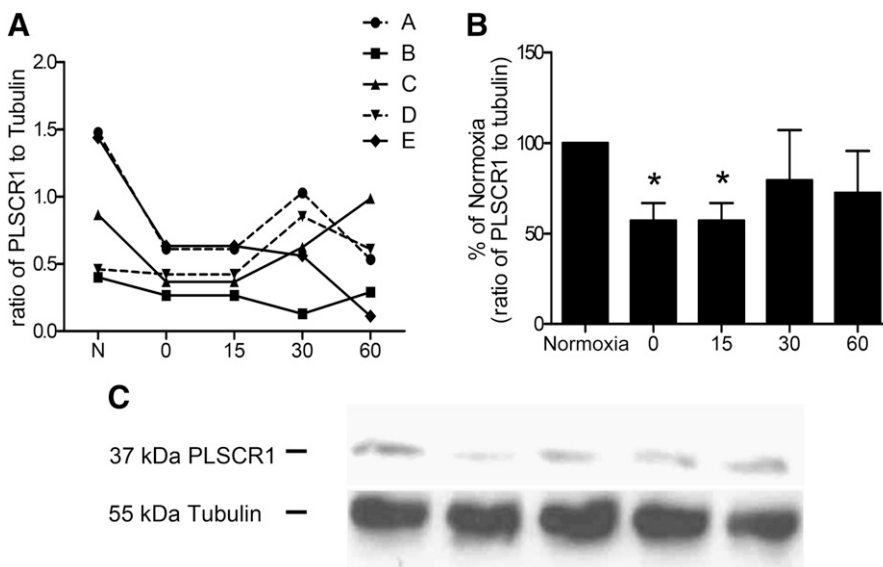


**Figure 5. PLSCR1 protein decreases with hypoxia in endothelial cells.** MS1 cells were subjected to 2 h of hypoxia (1% O<sub>2</sub>) followed by 0, 15, 30, or 60 min of normoxia or left in normal culture conditions (N). The 5 independent sets of lysates are presented in (A) as A, B, C, D, and E. The average of the 5 experiments are presented in (B). Whole cell lysates were prepared and run on SDS-PAGE followed by immunoblotting for PLSCR1 and the control protein tubulin. A representative blot is shown. ImageJ software (NIH) was used to quantify the bands, and a ratio of PLSCR1 to tubulin was determined.

activity under conditions of hypoxia and reoxygenation. NBD-PS was allowed to incorporate into endothelial cell membranes before the addition of NEM to chemically inhibit flippase activity. As shown in Fig. 6A–C, in the absence of NEM, NBD-PS was readily incorporated into the cell membranes, and no change in total (inner leaflet and outer leaflet) NBD-PS was observed after hypoxia or reoxygenation (Fig. 6A and C). However, quenching of NBD-PS in the outer leaflet by trypan blue revealed a statistically significant decrease in inner leaflet NBD-PS after hypoxia treatment (Fig. 6B and C). To evaluate the activity of PLSCR1 in the absence of flippase activity, additional cells were treated with NEM to chemically inhibit flippase activity. Although the addition of NEM

decreased overall NBD-PS incorporation, hypoxia and reoxygenation did not affect the total lipid incorporated (Fig. 6D and F). Furthermore, the increased translocation of NBD-PS from the inner to the outer leaflet present in the untreated cells (Fig. 6B and C) was also present in the NEM-treated cells (Fig. 6E and F). Thus, in endothelial cells, PLSCR1 activity is significantly increased by hypoxia and reoxygenation; the percentage of NBD-PS in the inner leaflet significantly decreases with hypoxia and reoxygenation compared with the percentage present in normoxia, indicating loss of NBD-PS from the inner leaflet (Fig. 6C). These data suggest that during hypoxia, PLSCR1 activity increases and translocates NBD-PS from the inner leaflet to the outer leaflet,

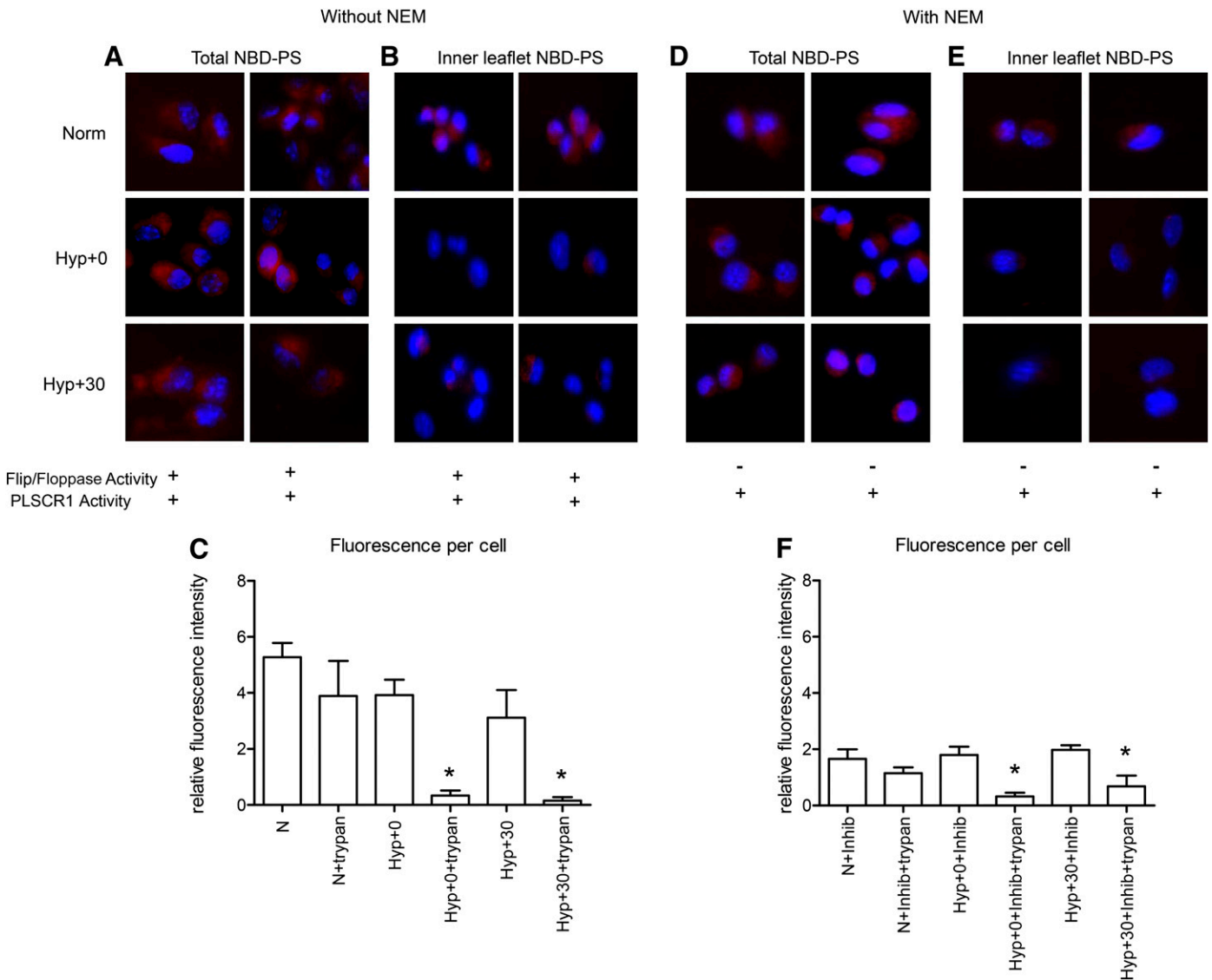


**Figure 6. PLSCR1 activity increases during hypoxia and reoxygenation.** Before normoxia (top row) or 2 h of hypoxia (1% O<sub>2</sub>) with or without 30 min of reoxygenation treatment, NBD-PS was incorporated into MSI cell membranes for 2 h with (D–F) or without (A–C) NEM treatment. Trypan blue was added to some of the samples to quench fluorescence in the outer leaflet (B and E). NBD-PS fluorescence is presented in red and nuclei in blue. The presence of NBD-PS both in the inner and outer leaflets and in the inner leaflet only (with trypan) in the presence (F) and absence (C) of NEM, are quantitated by ImageJ. Images are representative of 3 independent experiments with 3–6 pictures per treatment per experiment. \**P* < 0.05 compared with normoxia (N).

where it is quenched by trypan blue. PLSCR1 activity remains high during reoxygenation, because it continues to translocate NBD-PS.

### Knock down of PLSCR1 abrogates PS movement during hypoxia

To demonstrate a specific role for PLSCR1, the labeled lipid experiments were repeated after PLSCR1 expression was knocked down with siRNA. We hypothesized that if PLSCR1 was transporting NBD-PS across the membrane, knock down would limit the movement of NBD-PS and no difference would be observed in inner leaflet fluorescence across the treatments. Transfection resulted in knock down of *PLSCR1* to approximately 20% of that in the control transfected or untreated cells (Fig. 7A). Western blot analysis indicated PLSCR1 depletion in siRNA-treated cells compared with the control or untreated cells (Fig. 7B). Compared with the siRNA control-treated cells, knock down of *PLSCR1* did not alter the normoxic levels of steady-state *Cox2* mRNA but did significantly increase overall PGE<sub>2</sub> production (Fig. 7C and D). Similar to untreated cells, hypoxia induced a significant increase in both *Cox2* and PGE<sub>2</sub> in the control siRNA-treated cells. However, the hypoxia-induced increase was not found in *PLSCR1* siRNA-treated cells (Fig. 7C and D). Similar to the untreated cells in the previous experiment (Fig. 6), hypoxia treatment did not alter the total uptake of the lipid, as determined by the fluorescent signal in the control cells (Fig. 8A, C, and E). In addition, the inner leaflet fluorescent signal decreased with hypoxia treatment, suggesting movement from the inner leaflet to the outer leaflet by PLSCR1 (Fig. 8B and E). No change in inner leaflet fluorescence

occurred with hypoxia or hypoxia and reoxygenation when PLSCR1 was knocked down (Fig. 8D and E). No net movement of the lipid was detected in the absence of PLSCR1 (Fig. 8E). The data collected from the labeled lipid experiments suggests that PLSCR1 activity is increased during hypoxia and reoxygenation, allowing for the exposure of negatively charged phospholipids, such as PS, on the outer leaflet of the bilayer and production of lipid mediators such as PGE<sub>2</sub>.

### $\beta_2$ -GPI binding is decreased with knock down of PLSCR1

$\beta_2$ -GPI binding studies were performed to further support the hypothesis that PLSCR1 activity is required for  $\beta_2$ -GPI binding to the cell surface and initiating the inflammatory response. Endothelial cells in which PLSCR1 was knocked down with siRNA were used for these studies. Figure 9 shows that  $\beta_2$ -GPI binding is minimal when endothelial cells are kept in normoxic conditions but that hypoxia and reoxygenation treatment greatly enhance binding of  $\beta_2$ -GPI to untreated and control siRNA-treated cells. Hypoxia and reoxygenation treatment did not increase  $\beta_2$ -GPI binding on the cells in which PLSCR1 had been knocked down (Fig. 9).

Previous studies have demonstrated that natural IgM binds  $\beta_2$ -GPI and other neoantigens during reperfusion. To determine whether PLSCR1 plays a role in neoantigen expression after hypoxia, MS1 endothelial cells treated with control or PLSCR1 siRNA were subjected to hypoxia and reoxygenation in the presence of normal mouse serum. Under normoxic conditions, neither untreated, control, nor *PLSCR1* siRNA-treated cells stained positive for IgM (Fig. 10, top row). After

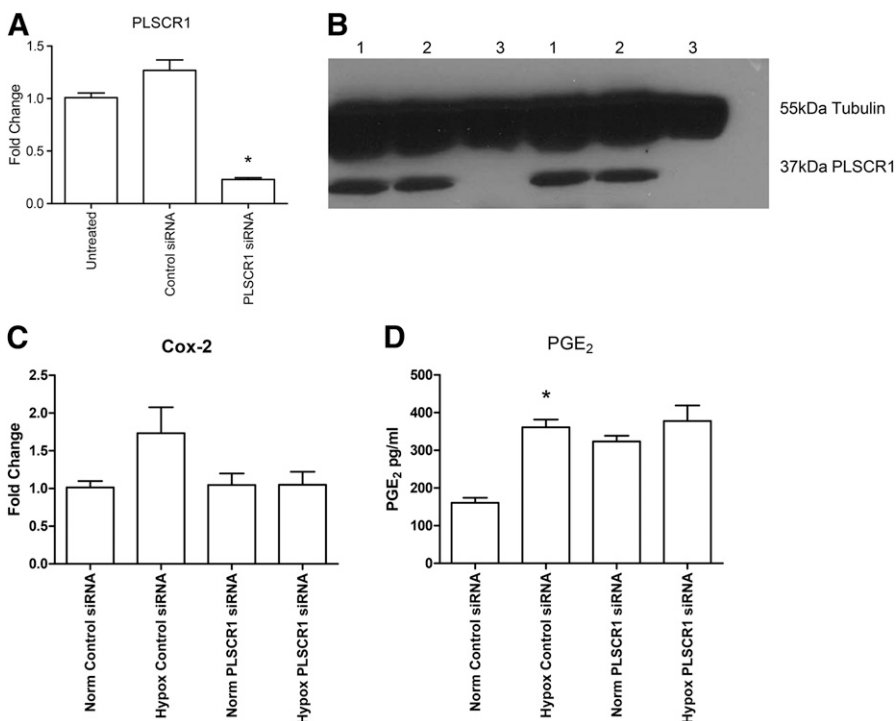


**Figure 7.** Hypoxia does not induce an increase in steady-state *Cox2* mRNA or PGE<sub>2</sub> production when MS1 cells are treated with PLSCR1 siRNA. MS1 endothelial cells were transfected with control or PLSCR1 siRNA before being subjected to normoxia or 2 h of hypoxia (1% O<sub>2</sub>). *PLSCR1* transcription of transfected MS1 cells was analyzed by QRT-PCR, as described in Materials and Methods (A), and PLSCR1 protein expression in cell lysates was determined by Western blot (B). After hypoxia or normoxia treatment, QRT-PCR determined *Cox2* steady-state mRNA expression in control or PLSCR1 siRNA-treated MS1 cells (C). After normoxia or hypoxia, PGE<sub>2</sub> secretions were determined from  $3 \times 10^5$  MS1 cells treated with control or PLSCR1 siRNA (D).  $N = 4$ –10 samples per bar from 2–3 experiments. \* $P < 0.05$  compared with respective control siRNA-treated cells.

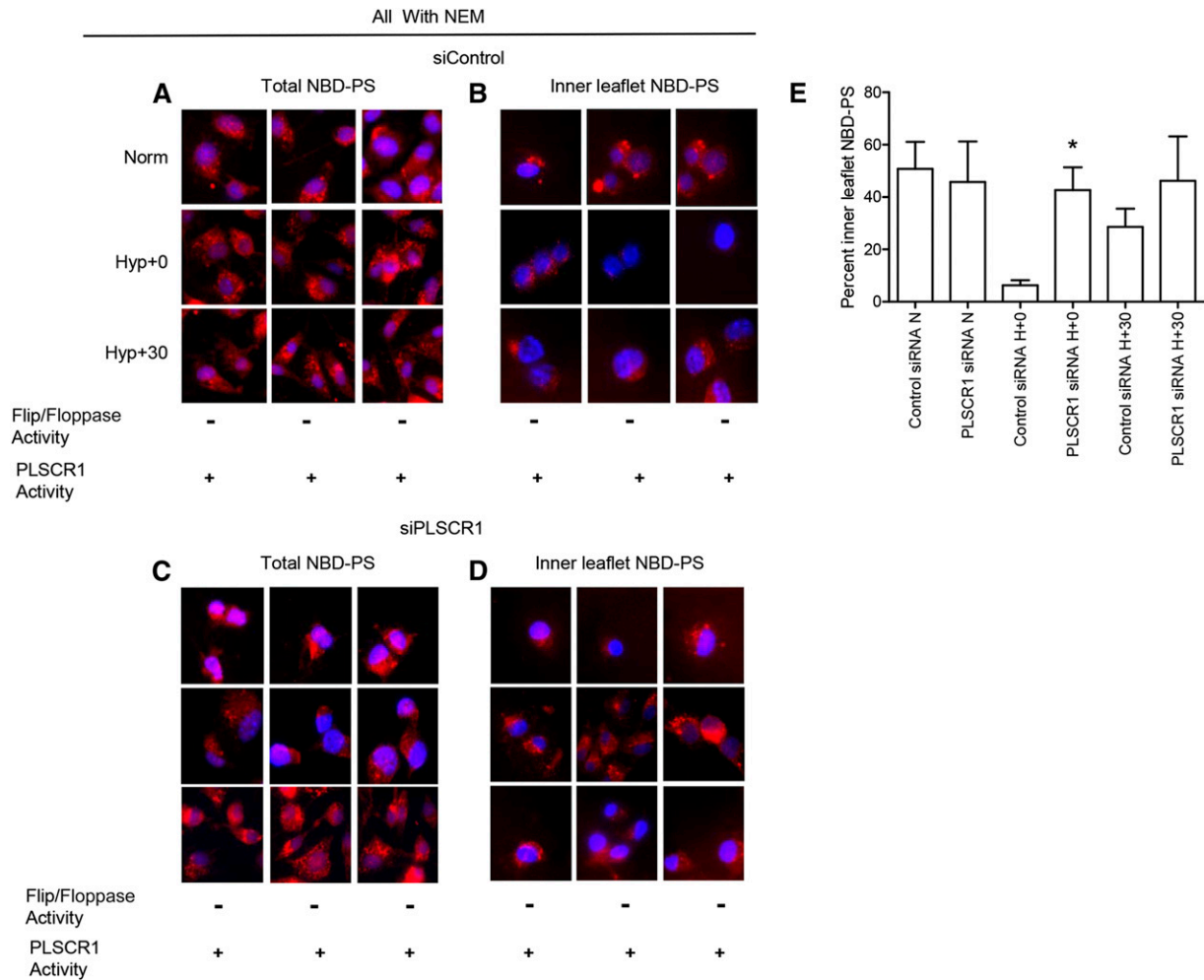


**Figure 8. PLSCR1 siRNA inhibits hypoxia-induced lipid translocation.** MS1 endothelial cells were transfected with control (A and B) or PLSCR1 (C and D) siRNA before subjection to normoxia (top row) or 2 h of hypoxia (1% O<sub>2</sub>) with or without 30 min of reoxygenation with NEM treatment. Trypan blue was added to additional samples to quench fluorescence in the outer leaflet (B and D). NBD-PS fluorescence is presented in red and nuclei in blue. NBD-PS in both the inner and outer leaflets (A and C) and in the inner leaflet only (B and D) of cells transfected with control siRNA (A and B) or PLSCR1 siRNA (C and D). Images (80 $\times$ ) are representative of 5 independent experiments with 3–6 pictures per treatment per experiment. ImageJ software (NIH) was used to quantify fluorescence (E). The percentage of fluorescence remaining in the inner leaflet after treatment is presented with 12–18 cells per treatment analyzed (E). \**P* < 0.05 compared with respective siRNA control.

hypoxia, IgM bound to untreated and control siRNA-treated cells but not to PLSCR1 siRNA-treated cells (Fig. 10, bottom row). No staining was visualized in the absence of normal mouse serum (data not shown). Together, these data further support our hypothesis that hypoxia and reoxygenation requires PLSCR1 activity for  $\beta_2$ -GPI and natural IgM binding to endothelial cell, possibly by inducing translocation of PS to the outer leaflet of the cell bilayer.

## DISCUSSION

Oxygen deprivation, whether acute or chronic, results in several changes at the cellular level. Stabilization of the HIF-1 $\alpha$  subunit allows for HIF activity, which alone influences the transcription of >150 genes (reviewed in [39, 40]). It is well established that inflammation contributes to IR-induced intestinal pathologic

features. However, the specific cell types involved and the specific role of HIF-1 $\alpha$  are unclear. For example, Kannan et al. [31] found partial HIF-1 $\alpha$  deficiency to be protective, but Hart et al. [41] found that HIF-1 $\alpha$  deficiency in intestinal epithelial cells enhanced intestinal IR-induced injury. We hypothesized that endothelial cells are key mediators of the lipid-mediated response observed after the oxygen deprivation that occurs with ischemia. Specifically, we hypothesized that lipid scrambling by PLSCR1 allows for PS exposure, which provides for binding of  $\beta_2$ -GPI, a serum protein, to endothelial cells and elicits cellular responses after hypoxia and reoxygenation. In the present study, we have demonstrated that subjecting endothelial cells to hypoxia and reoxygenation increases PLSCR1 activity and allows  $\beta_2$ -GPI binding to endothelial cells.

Preliminary studies were required to determine the optimal length of hypoxia treatment. Our goal was to ensure hypoxic conditions while preserving a high level of cell viability.

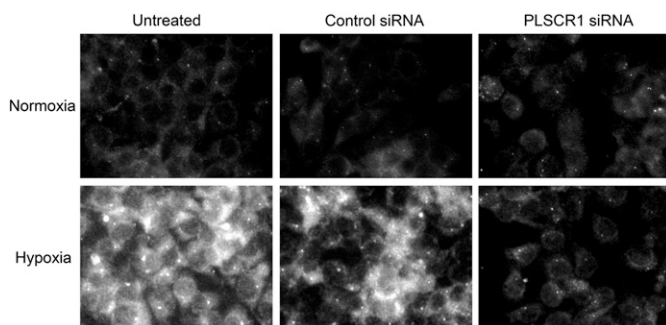


**Figure 9. PLSCR1 siRNA inhibits hypoxia-induced  $\beta_2$ -GPI binding to MS1 cells.** MS1 endothelial cells were untreated or transfected with control or PLSCR1 siRNA before subjection to normoxia (top row) or 2 h of hypoxia (1%  $O_2$ ) with 30 min of reoxygenation. The cells were fixed and stained with anti- $\beta_2$ -GPI. Images are representative of 3 independent experiments with 4–6 pictures per treatment group per experiment.

Although endothelial cells are sensitive to hypoxia, these cells release products required for the IR-induced inflammatory response. We found that 2 h of hypoxia at 1%  $O_2$  resulted in increased transcription of *HIF-1 $\alpha$* , as well as *VEGF* and *Flt-1* genes, directly induced by HIF [32, 33, 35], providing evidence that a state of hypoxia was attained. Exposure of the endothelial cells to hypoxia for >2 h significantly decreased cell viability (data not shown). These results are in agreement with those from Michiels et al., who also found 2 h of hypoxia to be optimal for primary human umbilical vein endothelial cells [42]. Because  $PGE_2$  production was significantly upregulated after hypoxia treatment, similar to the response observed from ex vivo intestinal tissue after IR [1, 3, 37], we continued our studies, exposing endothelial cells to 2 h of hypoxia.

This is the first comprehensive examination of the effects of hypoxia on PLSCR1 of which we are aware. Rami et al. performed immunohistochemical staining for PLSCR1 in human ischemic brain samples and found an increase in PLSCR1 protein in the ischemic samples compared with the controls [43]. Our data indicated a decrease in protein levels during a period of acute hypoxia (Fig. 5) but a significant increase in steady-state RNA on reoxygenation (Fig. 4A). The study by Rami et al. focused on the neurons of the brain, and our study examined endothelial cells in culture; thus, the differences in cell type and insult might resolve the apparent discrepancy. An additional factor to consider is the potential of PLSCR1 to be released from the membrane. The decreased protein expression found immediately after hypoxia treatment (Fig. 5) could have resulted from shedding of the protein into the culture medium, which was recently described for PLSCR3 [44].

PLSCR1 is a transmembrane protein when palmitoylated [45]; it facilitates scrambling of the lipid bilayer on an increase in intracellular calcium or other polycations [46]. Unlike flippases and floppases, PLSCR1 activity often abolishes membrane asymmetry, resulting in exposure of PE and PS on the outer leaflet (reviewed in [17]). Externalization of PS is a hallmark of apoptosis (reviewed in [12, 47]); however, transient exposure of PS is observed on cellular activation, coagulation [48], and

membrane blebbing [49].  $\beta_2$ -GPI, a serum protein, binds negatively charged phospholipids and has an affinity for PS [50]. Thus, several events might provide targets for  $\beta_2$ -GPI binding to the endothelium.

The role of PLSCR1 in PS translocation appears to vary depending on the context or purpose of the PS exposure. Initial studies of calcium-activated, PLSCR1 activation demonstrated that PLSCR1 translocated PS across the membrane but was not required for apoptosis-induced PS translocation or PS-induced coagulation when expressed on white blood cells or platelets, respectively (reviewed in [51]). Ory et al. demonstrated that although PLSCR1 is not required for exocytosis by lung epithelial cells, reinternalization of the vesicular membranes requires PLSCR1 [52]. Recent data have suggested that IFN- $\alpha$  activation of PLSCR1 might play a role in PS exposure and apoptosis, because ovarian cancer cell apoptosis increased when PLSCR1 expression was decreased [53]. Our data have demonstrated that hypoxia induces PS expression on the outer leaflet in a PLSCR1-dependent manner that is not sensitive to caspase inhibition (Fig. 3). Finally, we have demonstrated that PLSCR1 is required for natural antibody and the neoantigen  $\beta_2$ -GPI binding to endothelial cells in response to hypoxia (Figs. 9 and 10). Together, these studies support the hypothesis that PLSCR1 is activated during hypoxia and facilitates the movement of phospholipids between leaflets. PS expression as a result of IR-induced injury does not result in apoptosis, but rather necrosis, owing to complement-mediated cell death [54]. Thus, further studies are needed to determine whether the expression of other neoantigens and complement-mediated cell death require PLSCR1.

Recent studies have examined PLSCR1 levels in autoimmune patients, including APS and SLE patients. Transcription of PLSCR1 was found to be increased in blood monocytes of APS and SLE patients vs. controls [55, 56]. Interestingly,  $\beta_2$ -GPI is a common antigen for APS and SLE patients ([57], reviewed in [58]). Similarly, our data indicated increased PLSCR1 steady-state mRNA expression (Fig. 4A) and increased binding of  $\beta_2$ -GPI (Figs. 3 and 9) to endothelial cells with hypoxia and

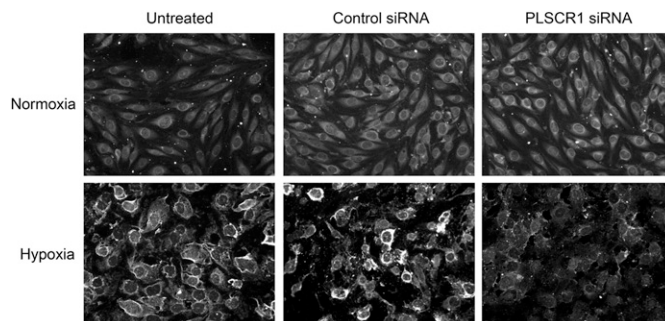


**Figure 10. PLSCR1 siRNA inhibits hypoxia-induced IgM binding to MS1 cells.** MS1 endothelial cells were untreated or transfected with control or PLSCR1 siRNA before subjection to normoxia (top row) or 2 h of hypoxia (1%  $O_2$ ) with 30 min of reoxygenation. Normal mouse serum (10%) was added to each well during normoxic and hypoxic conditions. The cells were washed, fixed, and stained with anti-IgM. Images are representative of 4–6 pictures per treatment group per experiment.

reoxygenation treatment. Furthermore, inflammation is common to APS, SLE, and IR-induced injury, supporting the hypothesis that PLSCR1-promoted  $\beta_2$ -GPI deposition is an early pathogenic change.

ESI-MS/MS analysis revealed few changes in the phospholipid composition of the endothelial cells with hypoxia treatment. LysoPC did increase with reoxygenation (Fig. 2A and Table 2), a trend also observed with hydrogen peroxide treatment of a human endothelial cell line [59]. Perhaps lysoPC production is a response coupled to oxidative damage, because both treatments result in such damage. Additionally, changes in AA were observed when endothelial cells were exposed to hydrogen peroxide [59].

The Cox1 isoform has traditionally been considered the constitutively active Cox enzyme, with inflammatory signals upregulating the Cox2 enzyme. Our data indicate an upregulation of steady-state mRNA of both isoforms (Fig. 2D–F). Additionally, the fold increase in transcription of *Cox1* was more than double that of *Cox2* ( $36.0 \pm 1.4$  vs.  $16.8 \pm 2.1$  at 30 min after hypoxia). North et al. similarly found an increase in Cox1 protein expression, but not Cox2 expression, at 15 min after exposure of primary pulmonary endothelial cells to low oxygen tension [60]. These results suggest that both isoforms could be involved in the downstream effects of hypoxic stress.

A time course tracking the effect of reoxygenation on PGE<sub>2</sub> production and secretion by endothelial cells revealed a peak at 30 min of reoxygenation after 2 h of hypoxia (Fig. 2F). Data from an in vitro study with bovine aortic endothelial cells and human umbilical vein endothelial cells complement our data (Fig. 2F), because an increase in total PGs was only observed after reoxygenation and not immediately after a hypoxic period of 2.5 h [61]. In vivo studies, which followed a similar time course, found the maximum PGE<sub>2</sub> response at 2 h after ischemia [1]. Several factors might contribute to this difference in the timing of maximal PGE<sub>2</sub> production and secretion. The hypoxic period in the present study was 2 h vs. 30 min of ischemia in vivo. The present study examined a single cell type (endothelium), but whole intestinal tissue, which consists of several cell types (including epithelium and smooth muscle, which are known to produce PGE<sub>2</sub> [62, 63]), was assessed in the previous study. Future studies are required to examine the PGE<sub>2</sub> produced by other cell types and combinations of different cell types [61].

Our in vitro model does lack the complexity and interactions that occur among cell types in whole tissue, in addition to the nutrient deprivation that occurs with IR. However, the endothelial cells used in our study yielded lipid-related changes similar to those obtained from whole tissue [1, 2, 37]. The endothelial cells produce and secrete vast quantities of PGE<sub>2</sub>, a vasodilator and driver of cellular permeability, in a short time period after relief of a hypoxic insult, another similarity to intestinal IR pathologic features [3]. Taken together, this cell model appears to be appropriate for future studies to determine whether the natural Ab recognition of other neoantigens and subsequent complement activation also occur on the endothelium.

The results we have presented provide an opportunity to further investigate several molecular interactions. First, the

relationship between PLSCR1 activity and PS exposure can be elucidated. It is possible that an indirect, rather than a direct, interaction occurs, potentially involving PGE<sub>2</sub> production, because the time points used in the present study could not be used to rule out the possibility that PS exposure or PLSCR1 transcription occurs secondary to PGE<sub>2</sub> production.

Several factors that contribute to IR-induced injury have been identified; however, few effective therapies are currently available. Our work has demonstrated that molecular events occurring in endothelial cells are relevant to the perpetuation of tissue injury. Lipid scrambling during hypoxia, via PLSCR1, allows for binding of IgM and the serum protein  $\beta_2$ -GPI on reoxygenation. It is currently unknown whether lipid changes result in expression of other neoantigens recognized by natural Abs, which in turn can trigger activation of the complement cascade in IR-induced injury. Additionally, lipid metabolism, including the generation of AA and subsequent conversion to PGE<sub>2</sub> via Cox enzymes, occurs. Thus, endothelial cells are a key factor in the initiation of multiple pathways leading to cellular damage and inflammation. Therefore, the role of PLSCR1 adds to the understanding of IR-induced pathogenesis and could provide a novel therapeutic target for surgical procedures.

## AUTHORSHIP

E.A.S. and S.D.F. conceived and designed the study. E.A.S. performed and analyzed most of the experiments. M.R.P. performed and analyzed the siRNA studies. E.A.S. and S.D.F. wrote the manuscript.

## ACKNOWLEDGMENTS

This work was supported by grants from the U.S. National Institutes of Health (NIH) Grants R01 AI061691, R21 AI107005 (to S.D.F.), and P20GM103418; the American Heart Association (to S.D.F.); and the Kansas State University National Science Foundation GK-12 program (to E.A.S.); and the Kansas State Confocal and Molecular Cores supported by Kansas State University College of Veterinary Medicine and Kansas State University. Any opinions, findings, and conclusions or recommendations expressed in the present study material are those of the authors and do not necessarily reflect the views of the NIH or National Science Foundation. The authors acknowledge Dr. Ruth Welti and Mary Roth (Kansas Lipidomics Research Center Analytical Laboratory, Kansas State University) for assistance with the lipid analysis.

## DISCLOSURES

The authors declare no competing financial interests.

## REFERENCES

1. Sparkes, B. L., Slone, E. E., Roth, M., Welti, R., Fleming, S. D. (2010) Intestinal lipid alterations occur prior to antibody-induced prostaglandin E2 production in a mouse model of ischemia/reperfusion. *Biochim. Biophys. Acta* **1801**, 517–525.
2. Slone, E. A., Pope, M. R., Roth, M., Welti, R., Fleming, S. D. (2012) TLR9 is dispensable for intestinal ischemia/reperfusion-induced tissue damage. *Am. J. Clin. Exp. Immunol.* **1**, 124–135.

3. Moses, T., Wagner, L., Fleming, S. D. (2009) TLR4-mediated Cox-2 expression increases intestinal ischemia/reperfusion-induced damage. *J. Leukoc. Biol.* **86**, 971–980.
4. Candelario-Jalil, E., González-Falcón, A., García-Cabrera, M., Alvarez, D., Al-Dalain, S., Martínez, G., León, O. S., Springer, J. E. (2003) Assessment of the relative contribution of COX-1 and COX-2 isoforms to ischemia-induced oxidative damage and neurodegeneration following transient global cerebral ischemia. *J. Neurochem.* **86**, 545–555.
5. Kishimoto, K., Li, R. C., Zhang, J., Klaus, J. A., Kibler, K. K., Doré, S., Koehler, R. C., Sapirstein, A. (2010) Cytosolic phospholipase A2 alpha amplifies early cyclooxygenase-2 expression, oxidative stress and MAP kinase phosphorylation after cerebral ischemia in mice. *J. Neuroinflammation* **7**, 42.
6. Watkins, M. T., Al-Badawi, H., Russo, A. L., Soler, H., Peterson, B., Patton, G. M. (2004) Human microvascular endothelial cell prostaglandin E1 synthesis during in vitro ischemia-reperfusion. *J. Cell. Biochem.* **92**, 472–480.
7. Schmedtje, J. F., Jr., Ji, Y. S., Liu, W. L., DuBois, R. N., Runge, M. S. (1997) Hypoxia induces cyclooxygenase-2 via the NF-kappaB p65 transcription factor in human vascular endothelial cells. *J. Biol. Chem.* **272**, 601–608.
8. Lang, P. A., Kasinathan, R. S., Brand, V. B., Durantou, C., Lang, C., Koka, S., Shumilina, E., Kempe, D. S., Tanneur, V., Akel, A., Lang, K. S., Foller, M., Kum, J. F., Kremser, P. G., Wesselborg, S., Laufer, S., Clemen, C. S., Herr, C., Noegel, A. A., Wieder, T., Gulbins, E., Lang, F., Huber, S. M. (2009) Accelerated clearance of Plasmodium-infected erythrocytes in sickle cell trait and annexin-A7 deficiency. *Cell. Physiol. Biochem.* **24**, 415–428.
9. Takayama, F., Wu, Z., Ma, H. M., Okada, R., Hayashi, Y., Nakanishi, H. (2013) Possible involvement of aiPLA2 in the phosphatidylserine-containing liposomes induced production of PGE2 and PGD2 in microglia. *J. Neuroimmunol.* **262**, 121–124.
10. Daleke, D. L. (2003) Regulation of transbilayer plasma membrane phospholipid asymmetry. *J. Lipid Res.* **44**, 233–242.
11. Fadeel, B., Xue, D. (2009) The ins and outs of phospholipid asymmetry in the plasma membrane: roles in health and disease. *Crit. Rev. Biochem. Mol. Biol.* **44**, 264–277.
12. Fadeel, B., Xue, D., Kagan, V. (2010) Programmed cell clearance: molecular regulation of the elimination of apoptotic cell corpses and its role in the resolution of inflammation. *Biochem. Biophys. Res. Commun.* **396**, 7–10.
13. Zwaal, R. F., Comfurius, P., Bevers, E. M. (2004) Scott syndrome, a bleeding disorder caused by defective scrambling of membrane phospholipids. *Biochim. Biophys. Acta* **1636**, 119–128.
14. Ioannou, Y., Zhang, J. Y., Passam, F. H., Rahgozar, S., Qi, J. C., Giannakopoulos, B., Qi, M., Yu, P., Yu, D. M., Hogg, P. J., Krilis, S. A. (2010) Naturally occurring free thiols within beta 2-glycoprotein I in vivo: nitrosylation, redox modification by endothelial cells, and regulation of oxidative stress-induced cell injury. *Blood* **116**, 1961–1970.
15. Passam, F. H., Qi, J. C., Tanaka, K., Matthaei, K. I., Krilis, S. A. (2010) In vivo modulation of angiogenesis by beta 2 glycoprotein I. *J. Autoimmun.* **35**, 232–240.
16. Manfredi, A. A., Rovere, P., Heltai, S., Galati, G., Nebbia, G., Tincani, A., Balestrieri, G., Sabbadini, M. G. (1998) Apoptotic cell clearance in systemic lupus erythematosus. II. Role of beta2-glycoprotein I. *Arthritis Rheum.* **41**, 215–223.
17. Contreras, F. X., Sánchez-Magraner, L., Alonso, A., Goñi, F. M. (2010) Transbilayer (flip-flop) lipid motion and lipid scrambling in membranes. *FEBS Lett.* **584**, 1779–1786.
18. Williamson, P., Kulick, A., Zachowski, A., Schlegel, R. A., Devaux, P. F. (1992) Ca2+ induces transbilayer redistribution of all major phospholipids in human erythrocytes. *Biochemistry* **31**, 6355–6360.
19. Williamson, P., Bevers, E. M., Smeets, E. F., Comfurius, P., Schlegel, R. A., Zwaal, R. F. (1995) Continuous analysis of the mechanism of activated transbilayer lipid movement in platelets. *Biochemistry* **34**, 10448–10455.
20. Bassé, F., Stout, J. G., Sims, P. J., Wiedmer, T. (1996) Isolation of an erythrocyte membrane protein that mediates Ca2+-dependent transbilayer movement of phospholipid. *J. Biol. Chem.* **271**, 17205–17210.
21. Stout, J. G., Bassé, F., Luhm, R. A., Weiss, H. J., Wiedmer, T., Sims, P. J. (1997) Scott syndrome erythrocytes contain a membrane protein capable of mediating Ca2+-dependent transbilayer migration of membrane phospholipids. *J. Clin. Invest.* **99**, 2232–2238.
22. Arnould, T., Michiels, C., Alexandre, I., Remacle, J. (1992) Effect of hypoxia upon intracellular calcium concentration of human endothelial cells. *J. Cell. Physiol.* **152**, 215–221.
23. Bouaziz, N., Redon, M., Quéré, L., Remacle, J., Michiels, C. (2002) Mitochondrial respiratory chain as a new target for anti-ischemic molecules. *Eur. J. Pharmacol.* **441**, 35–45.
24. Hattori, R., Otani, H., Moriguchi, Y., Matsubara, H., Yamamura, T., Nakao, Y., Omiya, H., Osako, M., Imamura, H. (2001) NHE and ICAM-1 expression in hypoxic/reoxygenated coronary microvascular endothelial cells. *Am. J. Physiol. Heart Circ. Physiol.* **280**, H2796–H2803.
25. Aono, Y., Ariyoshi, H., Sakon, M., Ueda, A., Tsuji, Y., Kawasaki, T., Monden, M. (2000) Human umbilical vein endothelial cells (HUVECs) show Ca(2+) mobilization as well as Ca(2+) influx upon hypoxia. *J. Cell. Biochem.* **78**, 458–464.
26. Toescu, E. C. (2004) Hypoxia sensing and pathways of cytosolic Ca2+ increases. *Cell Calcium* **36**, 187–199.
27. Zhou, Q., Zhao, J., Stout, J. G., Luhm, R. A., Wiedmer, T., Sims, P. J. (1997) Molecular cloning of human plasma membrane phospholipid scramblase: a protein mediating transbilayer movement of plasma membrane phospholipids. *J. Biol. Chem.* **272**, 18240–18244.
28. Devaiah, S. P., Roth, M. R., Baughman, E., Li, M., Tamura, P., Jeannotte, R., Welti, R., Wang, X. (2006) Quantitative profiling of polar glycerolipid species from organs of wild-type Arabidopsis and a phospholipase Dalp1a knockout mutant. *Phytochemistry* **67**, 1907–1924.
29. Bartz, R., Li, W. H., Venables, B., Zehmer, J. K., Roth, M. R., Welti, R., Anderson, R. G., Liu, P., Chapman, K. D. (2007) Lipidomics reveals that adiposomes store ether lipids and mediate phospholipid traffic. *J. Lipid Res.* **48**, 837–847.
30. Welti, R., Li, W., Li, M., Sang, Y., Biesiada, H., Zhou, H.-E., Rajashekar, C. B., Williams, T. D., Wang, X. (2002) Profiling membrane lipids in plant stress responses: role of phospholipase D alpha in freezing-induced lipid changes in Arabidopsis. *J. Biol. Chem.* **277**, 31994–32002.
31. Kannan, K. B., Colorado, I., Reino, D., Palange, D., Lu, Q., Qin, X., Abungu, B., Watkins, A., Caputo, F. J., Xu, D. Z., Semenza, G. L., Deitch, E. A., Feinman, R. (2011) Hypoxia-inducible factor plays a gut-injurious role in intestinal ischemia reperfusion injury. *Am. J. Physiol. Gastrointest. Liver Physiol.* **300**, G853–G861.
32. Liu, Y., Cox, S. R., Morita, T., Kourembanas, S. (1995) Hypoxia regulates vascular endothelial growth factor gene expression in endothelial cells. Identification of a 5' enhancer. *Circ. Res.* **77**, 638–643.
33. Namiki, A., Brogi, E., Kearney, M., Kim, E. A., Wu, T., Couffignal, T., Varticovski, L., Isner, J. M. (1995) Hypoxia induces vascular endothelial growth factor in cultured human endothelial cells. *J. Biol. Chem.* **270**, 31189–31195.
34. Levy, A. P., Levy, N. S., Wegner, S., Goldberg, M. A. (1995) Transcriptional regulation of the rat vascular endothelial growth factor gene by hypoxia. *J. Biol. Chem.* **270**, 13333–13340.
35. Gerber, H. P., Condorelli, F., Park, J., Ferrara, N. (1997) Differential transcriptional regulation of the two vascular endothelial growth factor receptor genes. Flt-1, but not Flk-1/KDR, is up-regulated by hypoxia. *J. Biol. Chem.* **272**, 23659–23667.
36. Zhao, L., Wu, Y., Xu, Z., Wang, H., Zhao, Z., Li, Y., Yang, P., Wei, X. (2012) Involvement of COX-2/PGE2 signalling in hypoxia-induced angiogenic response in endothelial cells. *J. Cell. Mol. Med.* **16**, 1840–1855.
37. Fleming, S. D., Pope, M. R., Hoffman, S. M., Moses, T., Bukovnik, U., Tomich, J. M., Wagner, L. M., Woods, K. M. (2010) Domain V peptides inhibit beta2-glycoprotein I-mediated mesenteric ischemia/reperfusion-induced tissue damage and inflammation. *J. Immunol.* **185**, 6168–6178.
38. Wurm, H. (1984) beta 2-Glycoprotein-I (apolipoprotein H) interactions with phospholipid vesicles. *Int. J. Biochem.* **16**, 511–515.
39. Majmundar, A. J., Wong, W. J., Simon, M. C. (2010) Hypoxia-inducible factors and the response to hypoxic stress. *Mol. Cell* **40**, 294–309.
40. Schofield, C. J., Ratcliffe, P. J. (2004) Oxygen sensing by HIF hydroxylases. *Nat. Rev. Mol. Cell Biol.* **5**, 343–354.
41. Hart, M. L., Grenz, A., Gorzolla, I. C., Schittenhelm, J., Dalton, J. H., Eltzhig, H. K. (2011) Hypoxia-inducible factor-1 $\alpha$ -dependent protection from intestinal ischemia/reperfusion injury involves ecto-5'-nucleotidase (CD73) and the A2B adenosine receptor. *J. Immunol.* **186**, 4367–4374.
42. Michiels, C., Arnould, T., Knott, I., Dieu, M., Remacle, J. (1993) Stimulation of prostaglandin synthesis by human endothelial cells exposed to hypoxia. *Am. J. Physiol.* **264**, C866–C874.
43. Rami, A., Sims, J., Botez, G., Winckler, J. (2003) Spatial resolution of phospholipid scramblase 1 (PLSCR1), caspase-3 activation and DNA-fragmentation in the human hippocampus after cerebral ischemia. *Neurochem. Int.* **43**, 79–87.
44. Inuzuka, T., Inokawa, A., Chen, C., Kizu, K., Narita, H., Shibata, H., Maki, M. (2013) ALG-2-interacting Tubby-like protein superfamily member PLSCR3 is secreted by an exosomal pathway and taken up by recipient cultured cells. *Biosci. Rep.* **33**, e00026.
45. Wiedmer, T., Zhao, J., Nanjundan, M., Sims, P. J. (2003) Palmitoylation of phospholipid scramblase 1 controls its distribution between nucleus and plasma membrane. *Biochemistry* **42**, 1227–1233.
46. Bucki, R., Giraud, F., Sulpice, J. C. (2000) Phosphatidylinositol 4,5-bisphosphate domain inducers promote phospholipid transverse redistribution in biological membranes. *Biochemistry* **39**, 5838–5844.
47. Ravichandran, K. S. (2011) Beginnings of a good apoptotic meal: the find-me and eat-me signaling pathways. *Immununity* **35**, 445–455.
48. Zwaal, R. F., Schroit, A. J. (1997) Pathophysiological implications of membrane phospholipid asymmetry in blood cells. *Blood* **89**, 1121–1132.
49. Kirov, A., Al-Hashimi, H., Solomon, P., Mazur, C., Thorpe, P. E., Sims, P. J., Tarantini, F., Kumar, T. K., Prudovsky, I. (2012) Phosphatidylserine

- externalization and membrane blebbing are involved in the nonclassical export of FGF1. *J. Cell. Biochem.* **113**, 956–966.
50. Agar, C., de Groot, P. G., Mörgelein, M., Monk, S. D., van Os, G., Levels, J. H., de Laat, B., Urbanus, R. T., Herwald, H., van der Poll, T., Meijers, J. C. (2011)  $\beta_2$ -glycoprotein I: a novel component of innate immunity. *Blood* **117**, 6939–6947.
  51. Bevers, E. M., Williamson, P. L. (2010) Phospholipid scramblase: an update. *FEBS Lett.* **584**, 2724–2730.
  52. Ory, S., Ceridono, M., Momboisse, F., Houy, S., Chasserot-Golaz, S., Heintz, D., Calco, V., Haeberlé, A. M., Espinoza, F. A., Sims, P. J., Bailly, Y., Bader, M. F., Gasman, S. (2013) Phospholipid scramblase-1-induced lipid reorganization regulates compensatory endocytosis in neuroendocrine cells. *J. Neurosci.* **33**, 3545–3556.
  53. Kodigepalli, K. M., Anur, P., Spellman, P., Sims, P. J., Nanjundan, M. (2013) Phospholipid scramblase 1, an interferon-regulated gene located at 3q23, is regulated by SnoN/SkiL in ovarian cancer cells. *Mol. Cancer* **12**, 32.
  54. Zhang, M., Hou, Y. J., Cavusoglu, E., Lee, D. C., Steffensen, R., Yang, L., Bashari, D., Villamil, J., Moussa, M., Fernaine, G., Jensenius, J. C., Marmur, J. D., Ko, W., Shevde, K. (2013) MASP-2 activation is involved in ischemia-related necrotic myocardial injury in humans. *Int. J. Cardiol.* **166**, 499–504.
  55. Amengual, O., Atsumi, T., Oku, K., Suzuki, E., Horita, T., Yasuda, S., Koike, T. (2013) Phospholipid scramblase 1 expression is enhanced in patients with antiphospholipid syndrome. *Mod. Rheumatol.* **23**, 81–88.
  56. Suzuki, J., Umeda, M., Sims, P. J., Nagata, S. (2010) Calcium-dependent phospholipid scrambling by TMEM16F. *Nature* **468**, 834–838.
  57. McNeil, H. P., Simpson, R. J., Chesterman, C. N., Krilis, S. A. (1990) Anti-phospholipid antibodies are directed against a complex antigen that includes a lipid-binding inhibitor of coagulation: beta 2-glycoprotein I (apolipoprotein H). *Proc. Natl. Acad. Sci. USA* **87**, 4120–4124.
  58. Alessandri, C., Conti, F., Pendolino, M., Mancini, R., Valesini, G. (2011) New autoantigens in the antiphospholipid syndrome. *Autoimmun. Rev.* **10**, 609–616.
  59. Yang, J., Yang, S., Gao, X., Yuan, Y. J. (2011) Integrative investigation of lipidome and signal pathways in human endothelial cells under oxidative stress. *Mol. Biosyst.* **7**, 2428–2440.
  60. North, A. J., Brannon, T. S., Wells, L. B., Campbell, W. B., Shaul, P. W. (1994) Hypoxia stimulates prostacyclin synthesis in newborn pulmonary artery endothelium by increasing cyclooxygenase-1 protein. *Circ. Res.* **75**, 33–40.
  61. Oudot, F., Cordelet, C., Sergiel, J. P., Grynberg, A. (1998) Polyunsaturated fatty acids influence prostanoid synthesis in vascular endothelial cells under hypoxia and reoxygenation. *Int. J. Vitam. Nutr. Res.* **68**, 263–271.
  62. Carew, M. A., Thorn, P. (2000) Carbachol-stimulated chloride secretion in mouse colon: evidence of a role for autocrine prostaglandin E2 release. *Exp. Physiol.* **85**, 67–72.
  63. Longo, W. E., Erickson, B., Panesar, N., Mazuski, J. E., Robinson, S., Kaminski, D. L. (1998) The role of selective cyclooxygenase isoforms in human intestinal smooth muscle cell stimulated prostanoid formation and proliferation. *Mediators Inflamm.* **7**, 373–380.

---

**KEY WORDS:**

Ischemia and reperfusion · apolipoprotein H · eicosanoids